The band structures of the silver halides AgF, AgCl, and AgBr: A comparative study

Stephan Glaus and Gion Calzaferri *

Department of Chemistry and Biochemistry, University of Berne, Freiestrasse 3, CH-3012 Bern, Switzerland. E-mail: gion.calzaferri@iac.unibe.ch; Fax: (+)31 6313994

The band structures of the silver halides AgX, X = F, Cl, and Br, which all form face centred cubic crystals are very similar. Especially the nature of the HOMO/LUMO region is similar. They differ somewhat in the band gap, in the dispersion of some bands and in the splitting between the 4d (Ag) and the np (X) levels and the ionicity which both are most pronounced in AgF. But their photochemical and chemical properties are very different. They are, to a large extent, controlled by surface properties (states) and by the secondary processes of the halides.

The importance of silver halides in the photographic process[1] and in electro- and photoelectrochemistry[2,3] are good reasons for a continued interest in these materials. The band structures of AgCl and AgBr are well understood but there remain some questions regarding the valence and the conduction band region of AgF[4]. We discuss this in a comparative study of AgF, AgCl and AgBr, which all form face centred cubic crystals. Main features of their band structures are a valence band maximum at the L-point and conduction band minima near the Γ-point. The distances in the silver halide series, the molecules and the crystals, behave similarly to those of the alkali halides, as seen in Table 1. The bandgap of the alkali and the silver halides shows less regularity. However, it is obvious that the bandgap of the alkali halides is much larger than that of the silver halides which varies in fact relatively little.

Silver halides have been subject of several different quantum chemical investigations. Calculations were started in the early sixties by Scop[11] and Bassani *et al.*[12]. Their work has already described the electronic properties of AgCl and AgBr well[13]. More sophisticated theoretical methods are now available, but usually problems in describing the bandgap properties have been observed. A recent example is a DFT study where the following bandgaps have been reported: 0 eV for AgF and 1 eV for AgCl and AgBr[14]. It seems that better values for more covalent bonding are obtained. The origin of the DFT failure for describing the electronic structure of charge transfer materials seems unfortunately not to be well understood. The problems are less severe for SCF-HF where after some corrections useful results but in this case too large bandgap energies have been reported for AgCl and AgF[15,16].

XPS photoelectron spectra of the silver halides AgBr, AgCl, and AgF have been reported by Mason[17]. We show them in Fig. 1. The largest peak at 4 to 5 eV can easily be assigned to the 4d(Ag) orbitals. But two additional peaks or shoulders on each side of the main band are observed. Going in the silver halide series from AgBr via AgCl to AgF, the peak at lower energy fades away and a shoulder remains in AgF. The peak at higher energy, which appears as shoulder in AgBr, grows. The assignment of these two features raised some controversies in the past, but in fact it appears to bear no mystery. The nature of the first electronic transition is the same for AgBr, AgCl, and AgF, namely an indirect Γ←L transition. Its value differs little but is a bit smaller in AgF and AgBr (2.8 ± 0.3 eV and 2.6 eV) than in AgCl (3.25 eV); see Table 2. XPS and ISS spectra for AgF and AgF$_2$ have been reported recently[18].

Table 1 Experimental distances in molecules and crystals and corresponding bandgaps

	d(AgX) molecule/Å	d(AgX) crystal/Å	Bandgap/eV
LiF	1.56[a]	2.01[b]	14.2[d]
LiCl	2.02[a]	2.57[b]	9.4[d]
LiBr	2.17[a]	2.78[b]	7.6[d]
NaF	1.93[a]	2.31[c]	11.5[d]
NaCl	2.36[a]	2.81[c]	9.0[d]
NaBr	2.50[a]	2.98[c]	7.1[d]
AgF	1.98[a]	2.47[e]	2.8 ± 0.3[e]
AgCl	2.28[a]	2.77[e]	3.25[f]
AgBr	2.39[a]	2.89[e]	2.69[f]

[a] Ref. 5 [b] Ref. 6 [c] Ref. 7 [d] Ref. 8 [e] Ref. 9 [f] Ref. 10
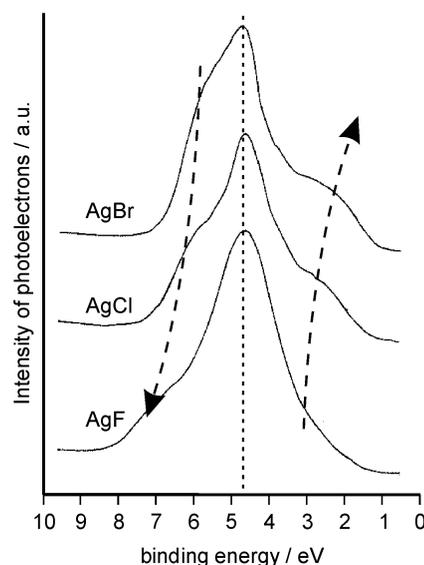
Fig. 1 XPS photoelectron spectrum of AgF, AgCl and AgBr.[17]

Differences in the band gap energies are sometimes estimated as follows. One would expect a smaller band gap when decreasing the unit cell constant. This is due to a shorter atom to atom distance which results in stronger interactions and hence a stronger splitting. Smaller sizes of the halides, the ionic radii, can compensate this effect. To get a comparable value we divide the sum of the corresponding ionic halide radius r(X⁻) and

Table 2 Experimental and theoretical values of AgF, AgCl, AgBr

Halide	Estimation Δ_E	Experiment				Calculation		
		Unit cell constant/Å	Ionic radius halide/Å	Indirect transition $\Gamma\leftarrow L$	Direct transition Γ	Indirect transition $\Gamma\leftarrow L$	Direct transition Γ	Charge/e
AgF	1.00	4.936[d]	1.17	2.8 ± 0.3[a]	4.63[a]	2.85	3.61	0.40
AgCl	1.06	5.54	1.67	3.25[b]	5.15[c]	3.28	5.28	0.12
AgBr	1.07	5.77	1.82	2.69[b]	4.29[c]	2.67	4.20	0.10

[a] Ref. 9 [b] Ref. 10 [c] Ref. 21 [d] Ref. 14
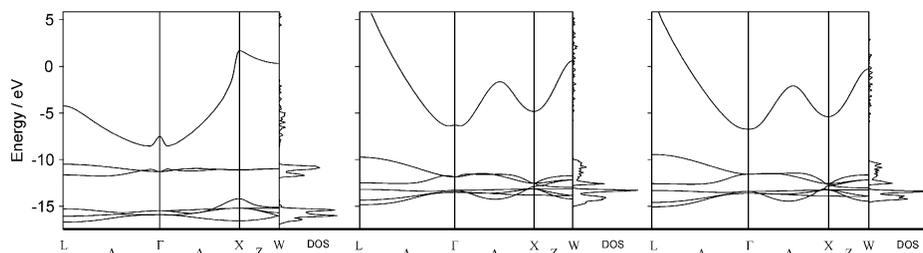
Fig. 2 Comparison of band structures and density of states of AgF (left) and AgCl (middle) and AgBr. The DOS of the valence band region is mainly composed of $np(X^-)$ levels while the DOS below has $4d(Ag^+)$ character

the ionic radius of a silver ion $r(Ag^+)$ which is 1.29 Å in an octahedral geometry by the unit cell constant $a(AgX)$ and multiply it by two.

$$\Delta_E = 2[r(X^-) + r(Ag^+)]/a(AgX) \qquad (1)$$

Table 2 left shows the result of this comparison. It is seen that the value of silver bromide and silver chloride is in the same range while silver fluoride shows a somewhat smaller value. This would lead us to expect that AgF has a larger band gap than AgCl and AgBr, which should lie in the same energy range. More insight can be gained by a band structure study. We use a EHTB type method (extended Hückel tight binding) because it was recently shown to give good results for AgCl[19,20]. Calculations of the band structures of AgF, AgCl, and AgBr have been carried out at the experimental geometries.

We show in Fig. 2 a comparison of the calculated band structures and the density of states (DOS) of the three silver halides. In all cases the first electronic transition is of indirect $\Gamma\leftarrow L$ type and the direct transition is located near or at the Γ point. This is in full agreement with the experimental data, as can be seen in Table 2. Even the fact that the energy of the indirect transition of AgF is a bit smaller than that of AgCl is reproduced. This should not be overemphasized, however, because small energy differences depend on small differences of bonding/antibonding interaction as e.g. explained in Fig. 4 of ref. 19. We observe that the calculated energy difference between the 2s(F) (not shown in the figure) and the 2p(F) band is 19.7 eV, this is in good agreement with the experimental value of 20.5 ± 0.4 eV[17]. A small local maximum appears at the Γ point of the conduction band for AgF. It nearly vanishes in AgCl and is absent in AgBr. At the Γ point of the conduction band no mixing between the s and p orbitals can occur for symmetry reasons. The antibonding interactions between the 5s(Ag) and the $ns(X)$ orbitals depends on the AgX distance. Hence it is strongest in AgF.

The shape of the AgF bands is similar to those of an AgCl and AgBr crystal although the calculation gives flatter bands for the AgF. No significant change of band ordering is observed. A typical change is the increasing dispersion and the increasing splitting mainly at L of the valence band, when going from AgF to AgBr. It is due to interaction of the $np(X^-)$ levels with the silver 4d levels. This hybridization was first noticed by Krumhansl[22]. It is, however, not sufficient to explain the smaller AgF bandgap with respect to AgCl. As shown in Fig. 2 the
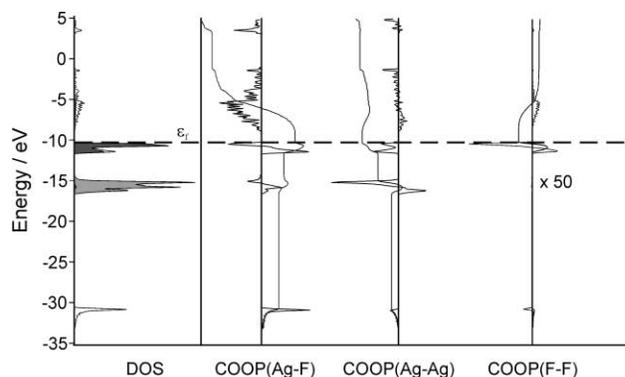
Fig. 3 Density of states (left) and contributions of the 4d(Ag) (light gray) and the 2p(F) (dark gray) orbitals as well as crystal orbital overlap populations of AgF.

conduction band of AgF lies at lower energy than in the two other halides. This is due to the stronger ionic character of AgF. The calculated charges are largest for AgF and about the same for AgBr and AgCl; see Table 2. While the absolute values are not of great significance, the relative values bear valuable information. The shape and position of the conduction band depends on the 5s(Ag) levels. The more positive charge on the silver ion in AgF results in a decrease of the 5s(Ag) Coulomb integrals: electrons in these orbitals will be more attracted and therefore stabilized. As a consequence the conduction band appears at lower energy.

We report some further details of the electronic structure of AgF in Fig. 3. The dashed horizontal line represents the Fermi level ε_F at -10.47 eV. The region below -30 eV is dominated by 2s(F) orbitals. The next region is characterized by the typical sharp features caused by the 4d(Ag) orbitals. The valence band region is dominated by 2p(F) orbitals. The integrated COOP (crystal orbital overlap population) is represented by the vertical dashed line. The bonding Ag–F interaction is only slightly weakened by an antibonding region just below the valence band edge. However the Ag–Ag and the F–F interactions are antibonding. Their integrated COOPs are both negative at the Fermi level. We refer to ref. 19 and references therein for a more detailed discussion of the COOP.

There is a thoroughgoing similarity in the band structures of the cubic AgF, AgCl and AgBr crystals. However, the chemical and photochemical activities of AgBr, AgCl and AgF are different. How can we understand this? The main reason is due

Table 3 Slater parameters for silver, fluorine, chlorine and bromine

Element	AO	ζ_1	ζ_2	c_1	c_2
F⁻	2s	2.425			
	2p	2.225			
Cl⁻	3s	2.700			
	3p	1.733			
Br⁻	4s	3.200			
	4p	2.131			
Ag⁺	5s	1.850			
	5p	1.300			
	4d	3.912	1.54	0.824	0.329

Table 4 SCCC parameters for silver, fluorine, chlorine and bromine

Silver	Configuration	d_2 (eV)	d_1 (eV)	d_0 (eV)
s VOIE	$4d^{10}5s^1$	0.5500	8.3900	7.5800
	$4d^9 5s^2$	0.3700	8.8800	8.8000
	$4d^9 5s^1 5p^1$	0.3100	9.7100	10.2300
p VOIE	$4d^{10}p^1$	0.7700	6.4600	3.8300
	$4d^9 p^2$	1.1800	6.8600	8.1200
	$4d^9 5s^1 5p^1$	1.1800	6.8600	4.7600
d VOIE	$4d^{10}$	−3.9000	25.6000	0.0000
	$4d^{10}5s^1$	0.4600	12.6600	12.7700
	$4d^{10}5p^1$	0.8100	11.6700	14.4900
Fluorine				
s VOIE	$2s^2 2p^5$	3.480	25.504	40.122
p VOIE	$2s^2 2p^5$	3.463	20.520	18.647
Chlorine				
s VOIE	$3s^2 3p^5$	1.699	15.709	25.268
p VOIE	$3s^2 3p^5$	1.673	13.180	13.688
Bromine				
s VOIE	$4s^2 4p^5$	1.699	15.709	22.070
p VOIE	$4s^2 4p^5$	1.673	13.180	13.100

to the fact that the observed reaction products are usually not formed by the primary processes but in consecutive reaction steps. This certainly applies for the differences in the photochemical behavior of AgCl and AgBr. While the former can be used as photocathode for water splitting, the latter is not suitable despite of the fact that both have similar valence bands. The reason is found in the different reactivities of the primary and secondary reaction products.[23] We also note the increase in covalency. It affects the surface properties of the materials which was investigated in some detail for AgCl[20] and AgBr[24,25] but not for AgF. The energy separation of the 2p(F) and the 4d(Ag) band in AgF was calculated to be larger than the corresponding separation in AgCl and AgBr. It is perhaps somewhat overestimated; however, the reason again originates in the higher ionicity of AgF. We conclude that this comparative study leads to a clear picture of the band structure of the silver halides with cubic structure which was missing so far.

Computational method

Extended Hückel tight-binding[26] band structure calculations were performed using BICON-CEDiT.[27] The off-diagonal elements were calculated by using the distance-dependent weighted Wolfsberg–Helmholtz formula[28]

$$H_{ij} = \frac{1}{2} K S_{ij}(H_{ij} + H_{ij}) \qquad (2)$$

$$K = 1 + k\left(\frac{\exp(-\delta(R - d_0))}{1 + (\delta(R - d_0 - |R - d_0|))^2}\right) \qquad (3)$$

with $\kappa = 0.8$, $\delta = 0.35$ Å⁻¹ and

$$k = \kappa\tau + \Delta^2 - \Delta^4\kappa; \quad \Delta = \frac{H_{ii} - H_{jj}}{H_{ii} + H_{jj}} \qquad (4)$$

R in eqn. (3) is the distance between the atoms and d_0 is the sum of the i-th and j-th orbital radii. The Slater exponents used and the parameters for the self-consistent charge procedure (SCCC), described in Ref. 20 are listed in Tables 3 and 4. The first Brillouin zone of a face centered cubic lattice with two atoms in the unit cell (Ag + halide) was used. The Γ point at the center of the zone possesses the highest symmetry, while Λ, Δ, and Z denote lines of high symmetry. Density of states (DOS) calculations have been carried out with a set of 56 k-points[29] representing the face centered cubic lattice.

References

1 T. H. James, *The Theory of the Photographic Process*, Macmillan: New York, 4th edn., 1977.
2 M. Lanz, D. Schürch and G. Calzaferri, Photocatalytic Oxidation of Water to O₂ on AgCl-coated Electrodes, *J. Photochem. Photobiol. A: Chem*, 1999, **120**, 105–117.
3 G. Calzaferri, D. Brühwiler, S. Glaus, D. Schürch, A. Currao and C. Leiggener, Quantum-Sized Silver, Silver Chloride and Silver Sulfide Clusters, *J. Imaging Sci. Technol.*, 2001, **45**, 331–339.
4 W. Grochala and R. Hoffmann, Real and hypothetical intermediate-valence Ag^{II}/Ag^{III} and Ag^{II}/Ag^{I} fluoride systems as potential superconductors, *Angew. Chem., Int. Ed. Engl.*, 2001, **40**(15), 2742–2781.
5 K. P. Huber, G. Herzberg, *Constants of Diatomic Molecules*; van Nostrand Reinhold Company: New York, 1979.
6 T. Asthalter and W. Weyrich, On the chemical interpretation of the one-electron density matrix of some ionic solids: LiH, LiF, and LiFHF, *Ber. Bunsen-Ges. Phys. Chem.*, 1997, **101**, 11–22; R. Marx and H. M. Mayer, Preparation and crystal structure of ordered and disordered lithium nitride dichloride, Li₅NCl₂, *J. Solid State Chem.*, 1997, **130**, 90–96; D. Doornhof, H. J. van Wijk and H. A. J. Oonk, Solid miscibility of common-anion lithium and sodium halides Experimental determination of the region of demixing in lithium bromide + sodium bromide, *Thermochim. Acta*, 1984, **76**, 171–178.
7 M. E. Straumanis, The refraction correction for lattice constants calculated from powder or rotation crystal patterns, *Acta Crystallogr.*, 1955, **8**, 654–655; W. H. Bragg, The Reflection of X-Rays by Crystals, *Proc. R. Soc. London, Ser. A.*, 1913, **89**, 246–248; Y. Pautamo, The temperature variation of volume and compressibility of solids, *Ann. Acad. Sci. Fenn. A VI*, 1963, **129**, 45.
8 A. B. Kunz, Study of the electronic structure of twelve alkali halide crystals, *Phys Rev B*, 1982, **26**((4)), 2056–2069.
9 A. P. Marchetti and G. L. Bottger, Optical Absorption Spectrum of AgF, *Phys. Rev. B.*, 1971, **3**((8)), 2604–2607.
10 F. C. Brown, *Solid State Chemistry*, edited by B. Hannay, Plenum, New York, 1973.
11 P. M. Scop, Band structure of silver chloride and silver bromide, *Phys. Rev. Sect. A*, 1965, **139**, 934–940.
12 F. Bassani, R. S. Knox and W. B. Fowler, Band Structure and Electronic Properties of AgCl and AgBr, *Phys. Rev. Sect. A*, 1965, **137**, 1217–1225.
13 R. H. Victora, Calculated electronic structure of silver halide crystals, *Phys. Rev. B*, 1997, **56**, 4417–4421.
14 B. N. Onwuagba, The electronics structure of AgF, AgCl, and AgBr, *Solid State Commun.*, 1996, **97**((4)), 267–271.
15 E. Aprà, E. Stefanovich, R. Dovesi and C. Roetti, An ab initio Hartree–Fock study of silver chloride, *Chem. Phys. Lett.*, 1991, **186**, 329–335.
16 A. B. Kunz, Electronic Structure of AgF, AgCl, and AgCl, *Phys Rev B*, 1982, **26**((4)), 2070–2075.
17 M. G. Mason, Photoelectron studies of the band structures of silver halides, *Phys. Rev. B*, 1975, **11**((12)), 5094–5102.
18 J. T. Wolan and G. B. Hoflund, Surface characterization study of AgF and AgF₂ powder using XPS and ISS, *Appl. Surf. Sci.*, 1998, **125**, 251–258.
19 S. Glaus and G. Calzaferri, Silver Chloride Clusters and Surface States, *J. Phys. Chem. B*, 1999, **103**, 5622–5630.
20 S. Glaus, G. Calzaferri and R. Hoffmann, Electronic Properties of

Silver-Silver Chloride Cluster Interfaces, *Chem. – Eur. J.*, 2002, **8**, 1785–1794.

21 B. L. Joesten and F.C. Brown, Indirect optical absorption of AgCl-AgBr alloys, *Phys. Rev.*, 1966, **148**, 919–927.

22 J. A. Krumhansl, Photoexcitation in ionic crystals, in *Photoconductivity Conference*, edited by R. G. Breckenridge, B. R. Russel, and E. E. Hahn, Wiley, New York, 1956.

23 D. Schürch, Antonio Currao, S. Sarkar, G. Hodes and G. Calzaferri, The Silver Chloride Photoanode in Photoelectrochemical Water Splitting, *J. Phys. Chem. B*, 2002, **106**, 12764–12775.

24 A.-S. Malik, F. J. DiSalvo, R. Hoffmann and J.T. Blair, A Detailed Theoretical Mechanism for Photographic Sensitization of the AgBr(111) Surface, *J. Imag. Sci. Technol.*, 1998, **42**((3)), 210–214.

25 R. C. Baetzold, Properties of Silver Clusters Adsorbed to Silver Bromide, *J. Phys. Chem. B*, 2001, **105**((17)), 3577–3586.

26 R. Hoffmann, An extended Hueckel theory. I. Hydrocarbons, *J. Chem. Phys.*, 1963, **39**, 1397–1412.

27 M. Brändle, R. Rytz, S. Glaus, G. Calzaferri, BICON-CEDiT, Extended Hückel Tight-Binding and Crystal Transition Dipole Moment Calculations, University of Bern, Switzerland, 2002, http://iacrs1.unibe.ch/Stephan.

28 D. Brühwiler, N. Gfeller and G. Calzaferri, Resorufin in the Channels of Zeolite L, *J. Phys. Chem. B*, 1998, **102**, 2923–2929.

29 A. H. MacDonald, Comment on special points for Brillouin-zone integrations, *Phys. Rev. B*, 1978, **18**, 5897–5899.